Enhancement of second harmonic generation (SHG) in ferrocene appended T-shaped chromophores: Impact of cyanovinylene moiety with TICT effect and theoretical insights

Vengidusamy Srinivasan Subiksha[a], P P Sanak Archana[a] and Nallasamy Palanisami[ab]*

[a]Department of Chemistry, School of Advanced Sciences, Vellore Institute of Technology, Vellore 632014, Tamil Nadu, India.

[b]Centre for Functional Materials, School of Advanced Sciences, Vellore Institute of Technology, Vellore 632014, Tamil Nadu, India.

E-mail: palanisami.n@gmail.com, palanisami.n@vit.ac.in Contact no: +91 98426 39776

1. Experimental

1.1 Materials and Methods

The required chemicals were purchased from Alfa Aesar, TCI, and Sigma Aldrich. The formation of the product was observed by thin layer chromatography (TLC) using commercially available TLC plates (silica gel Merck Co.). The pure product was attained by column chromatography, packed with silica gel (AVRA, 100-120 mesh). The solvents were used without prior purification. The starting material, 3,6-Diiodophthalanhydride was synthesized according to the previous reported procedure,[1] and the ferrocene phenyl boronic ester and ferrocene cyanovinylene phenyl boronic esters were synthesized from the reported literature.[2] Then, the *n*-butyl amine was substituted with 3,6-Diiodophthalanhydride by condensation reaction to yield the starting material 2-butyl-4,7-diiodoisoindoline-1,3-dione (**R1**). Finally, the T-shaped ferrocene phenyl conjugated 2-butyl-4,7-diiodoisoindoline-1,3-dione (**1**) and T-shaped ferrocene cyanovinylene substituted phenyl conjugated 2-butyl-4,7-diiodoisoindoline-1,3-dione (**2**) chromophores were synthesized by the Suzuki–Miyaura cross-coupling reaction.

1.2 General Physical Measurements

The BRUKER (400 MHz for ^{1}H and 100 MHz for ^{13}C NMR) spectrometer was used to record the NMR spectra using tetramethyl silane (TMS) as an internal standard, and deuterated chloroform (CDCl$_3$) served as the solvent. The chemical shifts were measured in ppm (δ). High-resolution mass spectra were recorded with the HRMS model Waters - Xevo G2- XS - QToF. A SHIMADZU IR Affinity-1 device fitted with a high-sensitivity DLATGS detector in ATR mode was used to obtain FT-IR spectra. Holmarc's Spin Coating unit, Model no: HO-TH-05C was utilized for the spin coating method. By dissolving the chromophores in CHCl$_3$ solvent, a JASCO UV-Visible spectrophotometer was used to record the absorption spectra in a 2 cm^2 quartz cuvette at room temperature. Tetrahydrofuran was used as a solvent by the Hitachi F-7000 FL spectrophotometer to get the fluorescence emission spectra. The electrochemical experimentations were conducted with a CHI620E model from CH-Instruments. The setup elaborate an oxygen-free single-compartment cell, utilizing a glassy carbon working electrode, a saturated Ag/AgCl reference electrode, and a platinum wire counter electrode. Chloroform was used as a solvent and [N(C$_4$H$_9$-*n*)$_4$] ClO$_4$ served as a supporting electrolyte. All E$_{1/2}$ values were calculated by (E_{pa} + E_{pc})/2 (E$_{pa}$ – anodic potential and E$_{pc}$ – cathodic potential) at a scan rate of 0.1 V s^{-1}. The thermogravimetric analysis (TGA) and differential scanning calorimetry (DSC) were measured using TGA SDT Q 600 V20.9

Build 20 instrument under nitrogen atmosphere by increasing the heat rate 20 $^{\circ}$C min^{-1} up to 800°C (0–800 $^{\circ}$C).

1.3 Single-Crystal X-ray Diffraction

The crystal measurements were carried out using CPAD based instrument named Bruker D8 QUEST PHOTON II diffractometer, which was equipped with an INCOATEC microfocus source with Mo radiation ($\lambda = 0.71073$ Å), and operating at 50 kV and 1.4 mA. The crystal was fixed on the glass loop with the approximate size of $0.04 \times 0.17 \times 0.28$ mm for chromophore **2**. The SADABS program was used to apply the absorption correction, and the SAINT program was used to integrate the diffraction profiles. Bruker SHELXTL used the full matrix least squares method using SHELXL-2019/1 to solve and refine the chromophore's structure.[3] APEX4 v2021.4-0 software was used to view the structure. For final data representation and structure plots, Olex2 software was used.

1.4 General Procedure for the Synthesis of Chromophores **1-2**

The ferrocenyl boronic ester and ferrocene cyanovinylene boronic ester were synthesized according to the previous literature.[2] Simultaneously, the 3,6-Diiodophthalanhydride was synthesized by referring to the reported literature,[1] followed by the condensation reaction with *n*-butyl amine in the presence of triethyl amine and toluene to yield the starting material **R1**. Finally, **R1** coupled with ferrocene phenyl boronic ester to synthesize chromophore **1**, and **R1** coupled with ferrocene cyano vinylene boronic ester to synthesize the chromophore **2** by Suzuki Miyara cross-coupling reaction using Pd(dppf)Cl$_2$ as a catalyst, potassium acetate base, and toluene solvent under N$_2$ atmosphere was reflexed for 12 hours. The pure product was obtained using column chromatography (hexane/ethyl acetate), displayed in Scheme S1.

1.4.1 **R1** (2-butyl-4,7-diiodoisoindoline-1,3-dione)

Half white solid, Yield: 60%, ^{1}H NMR (400 MHz, CDCl$_3$, δ, ppm): 7.66 (s, 2H, C$_6$H$_2$I$_2$), 3.63 (t, $J = 7.4$Hz, 2H, CH$_2$), 1.59 (m, 2H, CH$_2$), 1.32 (t, 2H, $J = 7.6$Hz, CH$_2$), 1.27 (t, $J = 3.6$Hz, 3H, CH$_3$). ^{13}C NMR (100 MHz, CDCl$_3$, δ, ppm): 165.1 (2C, C=O), 145.5 (2C, C$_6$H$_2$), 134.0 (2C, C$_6$H$_2$), 88.4 (2C, C-I), 38.5 (1C, CH$_2$), 30.3 (1C, CH$_2$), 20.1 (1C, CH$_2$), 13.6 (1C, CH$_3$). FT-IR (ATR) (cm^{-1}): 3066 (w) ν (C-H arom), 2947 (w) ν (C−H aliph), 1703 (s) ν (C=O), 1387 (s) ν (C=C), 1169 (s) ν (C-C) cm^{-1}. HR-mass for (C$_{12}$H$_{11}$I$_2$NO$_2$) (m/z); cald: 454.8879, found mass: 454.6138.

1.4.2 Chromophore **1 (**Bis ferrocene phenyl conjugated 2-butyl-4,7-diiodoisoindoline-1,3-dione)

Chromophore **1** is a yellow solid. Yield: 38%. ^{1}H NMR (400 MHz, CDCl$_3$, δ, ppm): 7.606 (s, 2H, C$_6$H$_2$), 7.51 (d, J = 8.4Hz, 4H, C$_6$H$_4$), 7.45 (d, 4H, J = 8.4Hz C$_6$H$_4$), 4.62 (s, 4H, C$_5$H$_4$), 4.28 (s, 4H, C$_5$H$_4$), 4.026 (s, 10H, C$_5$H$_5$), 3.56 (t, J = 7.2Hz 2H, CH$_2$), 1.56 (m, 2H, CH$_2$), 1.27 (m, 2H, CH$_2$), 0.83 (t, J = 7.2Hz, 3H, CH$_3$). ^{13}C NMR (100 MHz, CDCl$_3$, δ, ppm): 167.7 (2C, C=O), 140.0 (2C, C$_6$H$_4$), 139.5 (2C, C$_6$H$_2$), 135.7 (2C, C$_6$H$_2$), 133.8 (2C, C$_6$H$_2$), 129.5 (2C, C$_6$H$_4$), 128.3 (4C, C$_6$H$_4$), 125.7 (4C, C$_6$H$_4$), 84.8 (2C, C$_{ipso}$ C$_5$H$_5$), 69.7 (10C, 2C$_5$H$_4$), 69.4 (4C, 2C$_5$H$_4$), 66.7 (4C, 2C$_5$H$_4$), 37.8 (1C, CH$_2$), 30.5 (1C, CH$_2$), 20.2 (1C, CH$_2$), 13.6 (1C, CH$_3$). FT-IR (ATR) (cm^{-1}): 3092 (w) ν (C-H arom), 2943 (w) ν (C−H aliph), 1708 (s) ν (C=O), 1400 (s) ν (C=C), 1105 (s) ν (C-C), 810 (s) ν (C=C Fc) cm^{-1}. Elemental analyses [CHN] (C$_{44}$H$_{37}$Fe$_2$NO$_2$): Calcd. C, 73.05; H, 5.16; N, 1.94, found C, 73.37; H, 5.19; N, 1.74. HR-mass for (C$_{44}$H$_{37}$Fe$_2$NO$_2$) (m/z); cald: 723.1523, found mass: 723.1514, UV-Visible data λ$_{max}$ (CH$_2$Cl$_2$) (nm): 275 (π-π*), 360 (n-π*), 458 (d-d), λ$_{max}$ (Thin film) (nm): 281 (π-π*), 319 (n-π*), 464 (d-d). Fluorescence data, excitation λ$_{ex}$ (THF) = 280 nm, emission λ$_{em}$ = 419 nm, excitation λ$_{ex}$ (Thin film) = 280 nm, emission λ$_{em}$ = 400 nm.

1.4.3 Chromophore **2 (**Bis ferrocene cyanovinylene substituted phenyl conjugated 2-butyl-4,7-diiodoisoindoline-1,3-dione)

Chromophore **2** is a dark red color solid, recrystallized using deuterated chloroform. Yield: 42%. ^{1}H NMR (400 MHz, CDCl$_3$, δ, ppm): 7.67 (d, J = 8.4Hz, 4H, C$_6$H$_4$), 7.625 (s, 2H, C$_6$H$_2$), 7.57 (d, J = 8.4Hz, 4H, C$_6$H$_4$), 7.43 (s, 2H, CH), 4.94 (s, 4H, C$_5$H$_4$), 4.50 (s, 4H, C$_5$H$_4$), 4.19 (s, 10H, C$_5$H$_5$), 3.56 (t, J = 7.2Hz 2H, CH$_2$), 1.57 (m, 2H, CH$_2$), 1.27 (m, 2H, CH$_2$), 0.83 (t, J = 7.4Hz, 3H, CH$_3$). ^{13}C NMR (100 MHz, CDCl$_3$, δ, ppm): 167.5 (2C, C=O), 144.1 (2C, CH), 141.1 (2C, C$_6$H$_4$), 139.1 (2C, C$_6$H$_4$), 135.9 (2C, C$_6$H$_4$), 135.7 (2C, C$_6$H$_4$), 130.2 (2C, C$_6$H$_2$), 128.5 (2C, C$_6$H$_4$), 126.6 (2C, C$_6$H$_2$), 124.7 (2C, C$_6$H$_2$), 119.3 (1C, CN), 119.0 (1C, CN), 116.0 (2C, C$_6$H$_4$), 106.4 (1C, C=C-CN), 105.9 (1C, C=C-CN), 77.8 (2C, C$_{ipso}$ C$_5$H$_5$), 71.8 (5C, C$_5$H$_5$), 71.2 (5C, C$_5$H$_5$), 70.3 (4C, 2C$_5$H$_4$), 69.9 (2C, 2C$_5$H$_4$), 69.7 (2C, 2C$_5$H$_4$) , 37.9 (1C, CH$_2$), 29.7 (1C, CH$_2$), 20.2 (1C, CH$_2$), 13.6 (1C, CH$_3$). FT-IR (ATR) (cm^{-1}): 3027 (w) ν (C-H arom), 2947 (w) ν (C−H aliph), 2203 (w) ν (C ≡N), 1708 (s) ν (C=O), 1387 (s) ν (C=C), 1062 (s) ν (C-C), 815 (s) ν (C=C Fc) cm^{-1}. Elemental analyses [CHN] (C$_{50}$H$_{39}$Fe$_2$N$_3$O$_2$): Calcd. C, 72.74; H, 4.76; N, 5.09, found C, 72.37; H, 4.48; N, 4.96. HR-mass for (C$_{50}$H$_{39}$Fe$_2$N$_3$O$_2$) (m/z); cald: 825.1741, found mass: 825.1748, UV-Visible data λ$_{max}$ (CH$_2$Cl$_2$) (nm): 274 (π-π*), 376 (n-π*), 505 (d-d), λ$_{max}$ (Thin film) (nm) 287 (π-π*), 348 (n-π*), 474 (d-d). Fluorescence data,

excitation λ_{ex} (THF) = 280 nm, emission λ_{em} = 417 nm. excitation λ_{ex} (Thin film) = 280 nm, emission λ_{em} = 401 nm.

1.5 Cyclic Voltammetry (CV)

The redox potential obtained from CV is used to calculate the half wave potential and energy gap of the chromophores using the following equations, Eqn. 5.1 and Eqn. 5.2[4]

$$E_{1/2} = (E_{pa} + E_{pc})/2 \tag{1}$$

$$\Delta E = E_{pa} - E_{pc} \tag{2}$$

Where, E_{pa} (anodic potential), i_a (anodic current), E_{pc} (cathodic potential), i_c (cathodic current), $E_{1/2}$ (half-wave potential) and ΔE (peak separation).

1.6 NLO Measurements (SHG)

The SHG efficiency of the chromophores **1-2** were obtained from the Kurtz and Perry powder technique using Ti:Sapphire laser with a fundamental wavelength of 800 nm.[5] The ground samples with an approximate particle size of 80 μm were taken in a glass capillary tube and covered with tape 1 mm thick and aluminum holders containing an 8 mm diameter hole. The potassium dihydrogen phosphate (KDP) was used as a reference material for the measurement. The Ti Sapphire laser-producing pulses with a width of 8 ns and a repetition rate of 10 Hz were used in this study. The laser beam was passed through an IR reflector and then directed to the sample holder. The incident optical signal in PMT was converted into voltage output.

1.7 Computational Calculation

The density functional theory (DFT) calculations were functioned to confirm the structural and electronic features of the chromophores. The bonding pattern, electronic charge, and molecular orbital energy distributions were well-defined through the help of the combination of B3LYP with the 6-31+G** basis set for entire calculations.[6] The single-excitation configuration interaction technique combined with the time-dependent DFT (TD-DFT) method is utilized to calculate the dipole moments for the NLO active chromophores at the excited state, which helps to investigate the origin of electronic absorption spectra and nonlinear optical properties. The geometries of the T-shaped bi-ferrocenyl *n*-butylamine substituted indanedione and bi-ferrocenyl *n*-butylamine and cyanovinylene substituted indanedione chromophores were optimized, and electrostatic potential mapping were developed. Further, dipole moment, polarizability and first hyperpolarizability was calculated using B3LYP/6–31+G**. All the

5

computational studies were done in Gaussian 16 package.[7] The Gauss View 6.1.1 molecular visualization tool provided the electronic geometries and frontier molecular orbital configurations. The efficiency of dipole moment (μ), polarizability (α_o) and first hyperpolarizability (β_0) of the chromophores were depends upon the electronic transition between donor and acceptor through π-conjugator, which were calculated using B3LYP combined with the 6-31+G** basis set and the values were reported in the atomic mass units (a.u) and electrostatic unit (esu). The β component was defined as the coefficients in the Taylor series expansion of the energy in the external electric field. If the external electric field is weak and homogeneous, then the expansion becomes as follows.

$$E = E^0 - \mu_\alpha F_\alpha - 1/2\alpha_\alpha\beta F_\alpha F_\beta - 1/6\beta_\alpha\beta_\gamma F_\alpha F_\beta F_\gamma + \ldots\ldots\ldots\ldots (3)$$

Hence, E_0 is the energy of the unperturbed molecules, F_α is the field at the rigid, μ_α, $\alpha_{\alpha\beta}$ and $\beta_\alpha\beta_\gamma$ are the components of dipole moment, polarizability and the first order hyperpolarizabilities respectively. The magnitude of total static dipole moment (μ_{tot}), the mean polarizability (α_o) and the mean first hyperpolarizability (β_o) were calculated by referring the literature.[9] The mean polarizability was defined as the following equation,

$$\alpha_o = (\alpha_{xx} + \alpha_{yy} + \alpha_{zz})/3 \ldots\ldots\ldots\ldots (4)$$

The components of the first hyperpolarizability can be calculated by the following equation.

$$\beta_0 = (\beta^2_x + \beta^2_y + \beta^2_z)^{1/2} \ldots\ldots\ldots\ldots (5)$$

Where, $\beta_x = \beta_{xxx} + \beta_{yyy} + \beta_{zzz}$; $\beta_y = \beta_{yyy} + \beta_{yzz} + \beta_{yxx}$; $\beta_z = \beta_{zzz} + \beta_{zxx} + \beta_{zyy}$ is used to calculate the magnitude of β_0. The total dipole moment can be calculated using the equation. (6)

$$\mu_t = (\mu_x^2 + \mu_y^2 + \mu_z^2)^{1/2} \ldots\ldots\ldots\ldots (6)$$

1.8 Synthesis

The precursor (**R1**) was synthesized by condensation reaction using *n*-butyl amine and 3,6-diiodo phthalic anhydride in triethyl amine and toluene at 110 °C. The reaction was refluxed for 5 hours and the pure product was obtained using column chromatography (hexane/ethyl acetate). Then, **R1** was coupled with ferrocene phenyl boronic ester (Chromophore **1**) and ferrocene cyano vinylene boronic ester (Chromophore **2**) by Suzuki-Miyaura reaction to yield the final products **1** and **2** (Scheme S1).
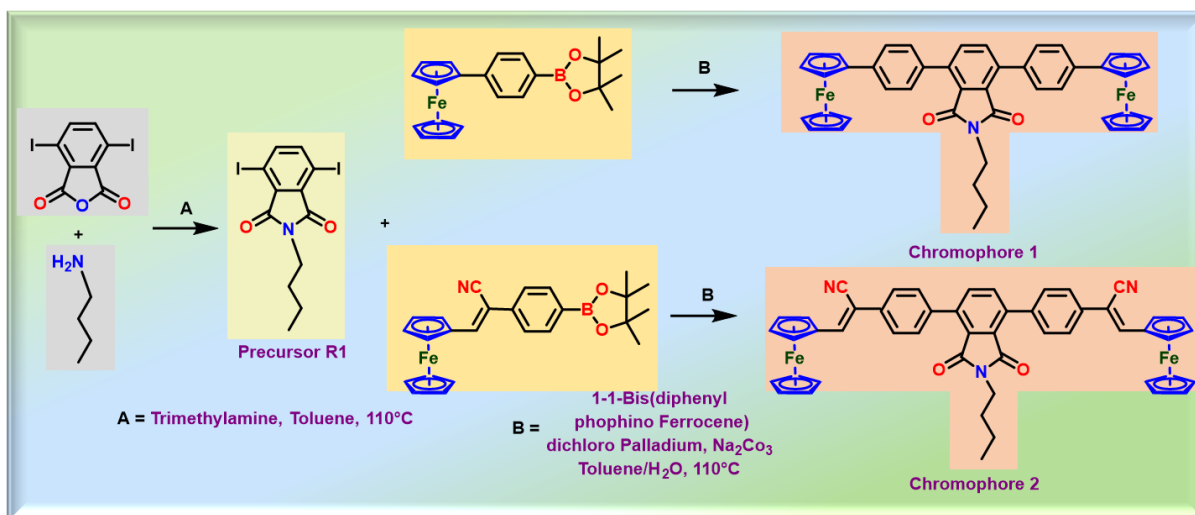
Scheme S1 The synthetic route for the synthesis of chromophores **1** and **2**
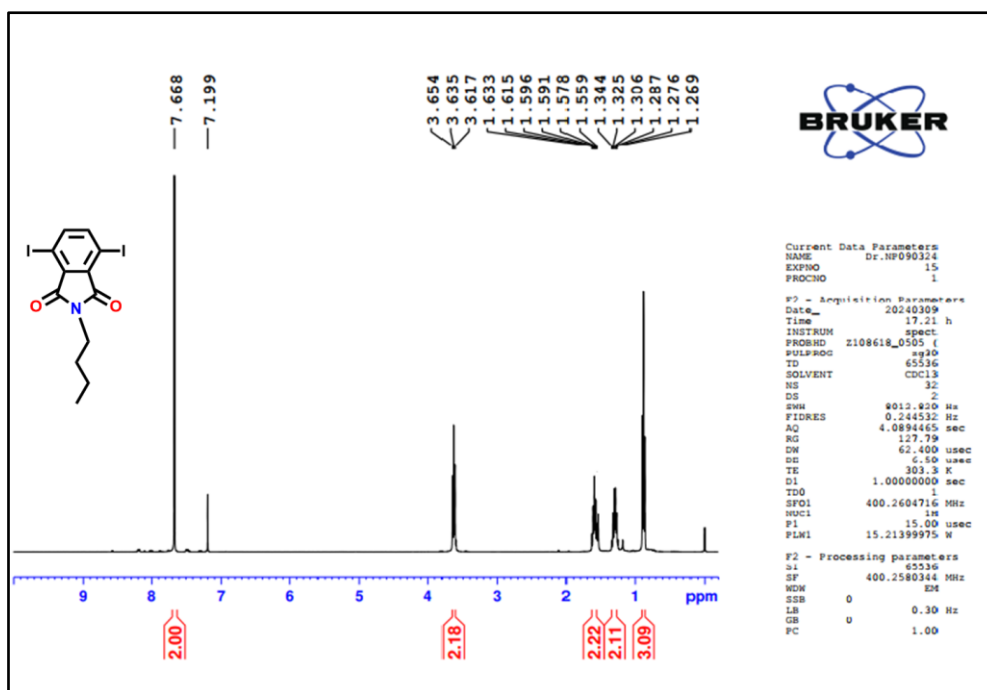
Fig. S1 ^{1}H NMR spectra of the precursor **R1** in CDCl$_3$ at 27°C
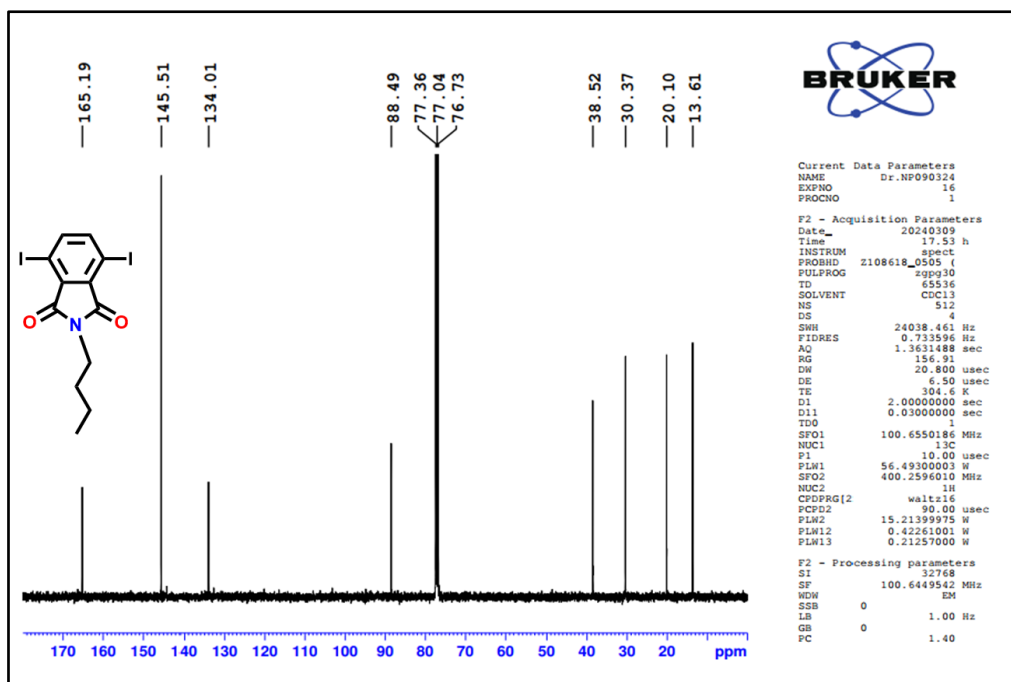
Fig. S2 ^{13}C NMR spectra of the precursor **R1** in CDCl$_3$ at 27°C

Fig. S3 ^{1}H NMR spectra of the chromophore **1** in CDCl$_3$ at 27°C

8

Fig. S4 ^{13}C NMR spectra of the chromophore **1** in CDCl$_3$ at 27°C
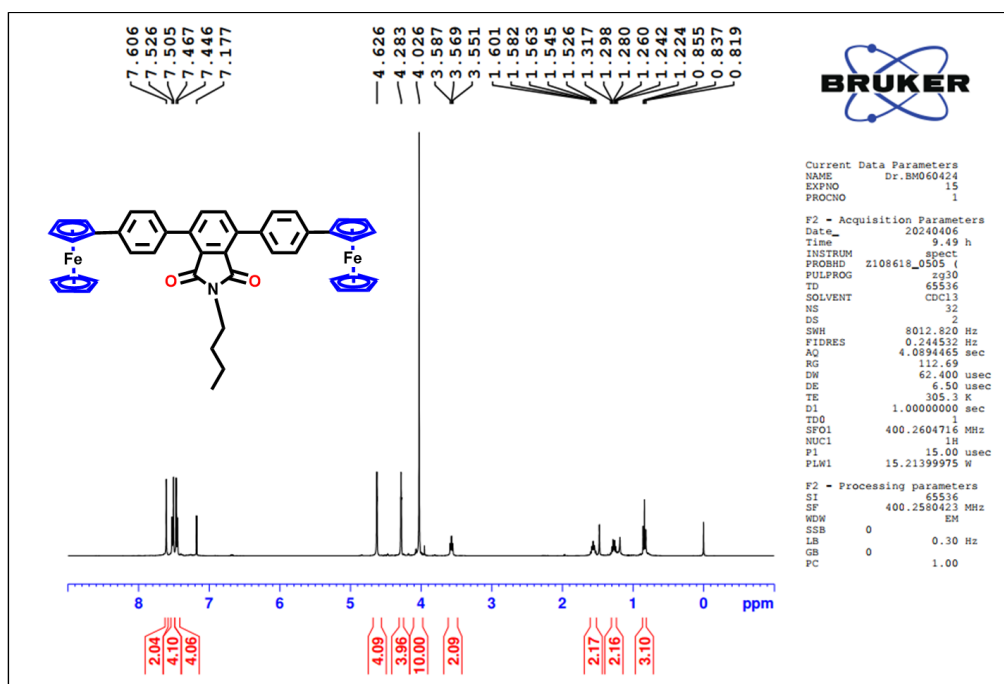
Fig. S5 ^{1}H NMR spectra of the chromophore **2** in CDCl$_3$ at 27°C
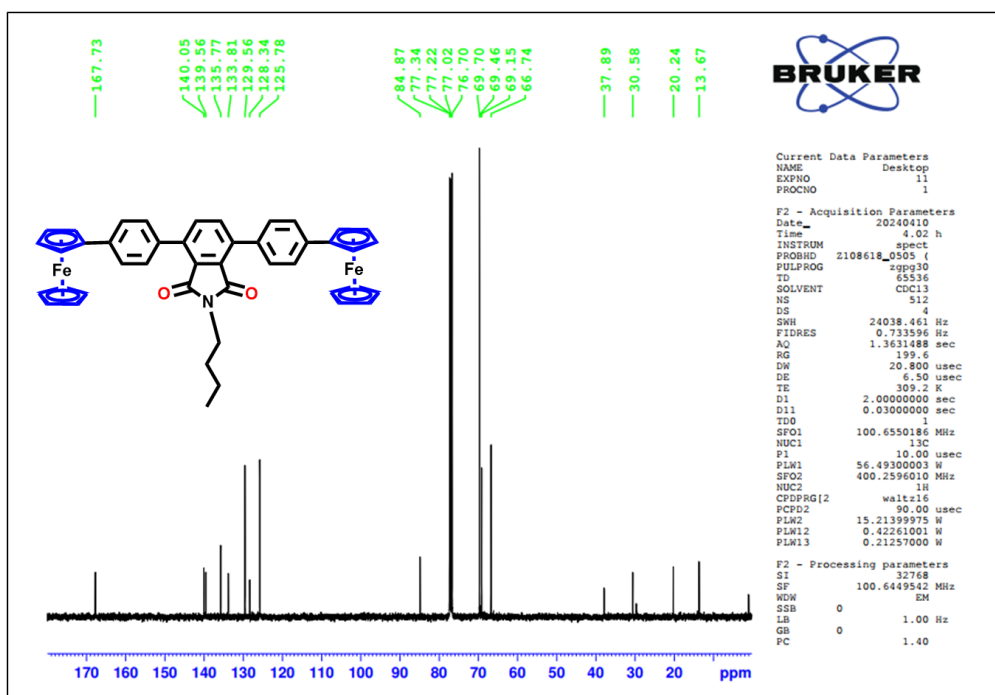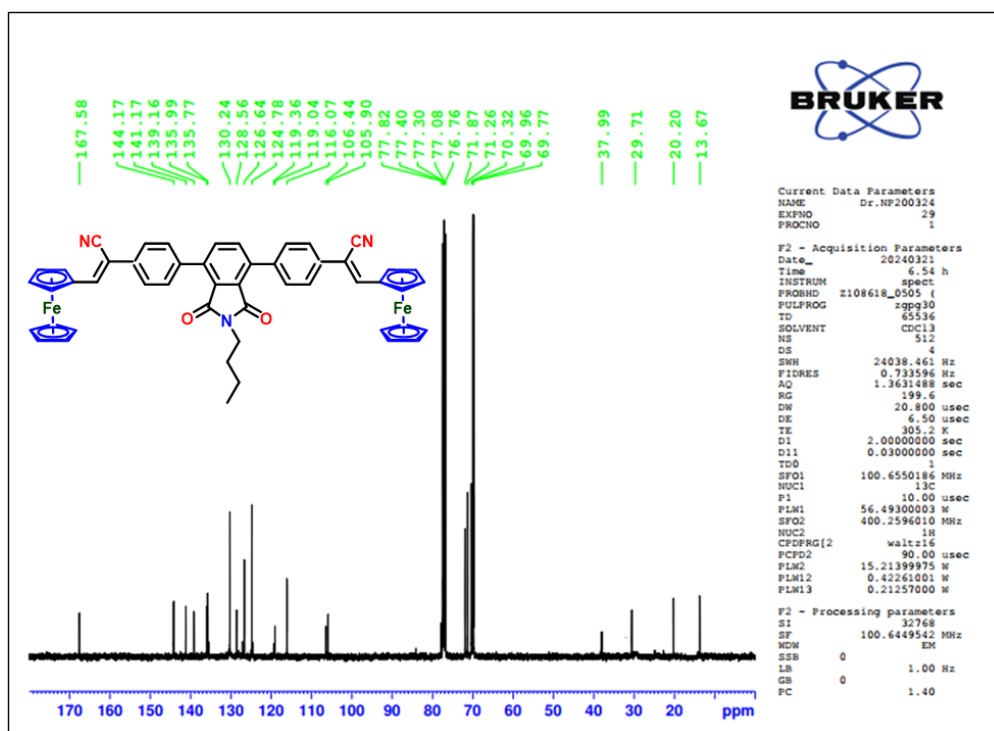
Fig. S6 ^{13}C NMR spectra of the chromophore **2** in CDCl$_3$ at 27°C
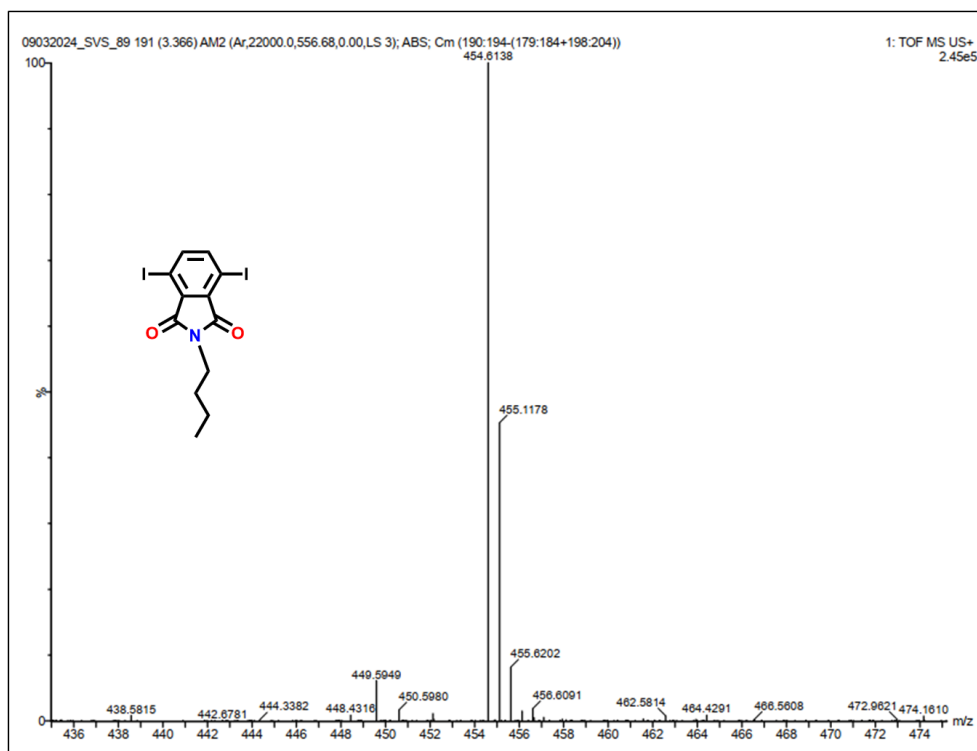
Fig. S7 HR-Mass spectra of the precursor **R1**
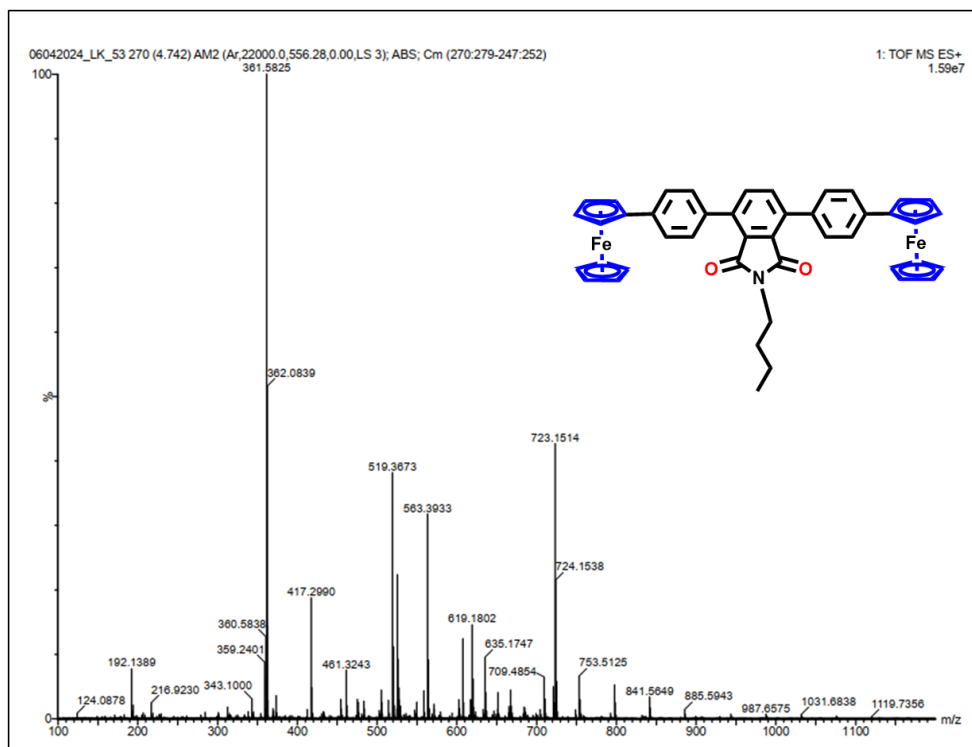
Fig. S8 HR-Mass spectra of the chromophore **1**
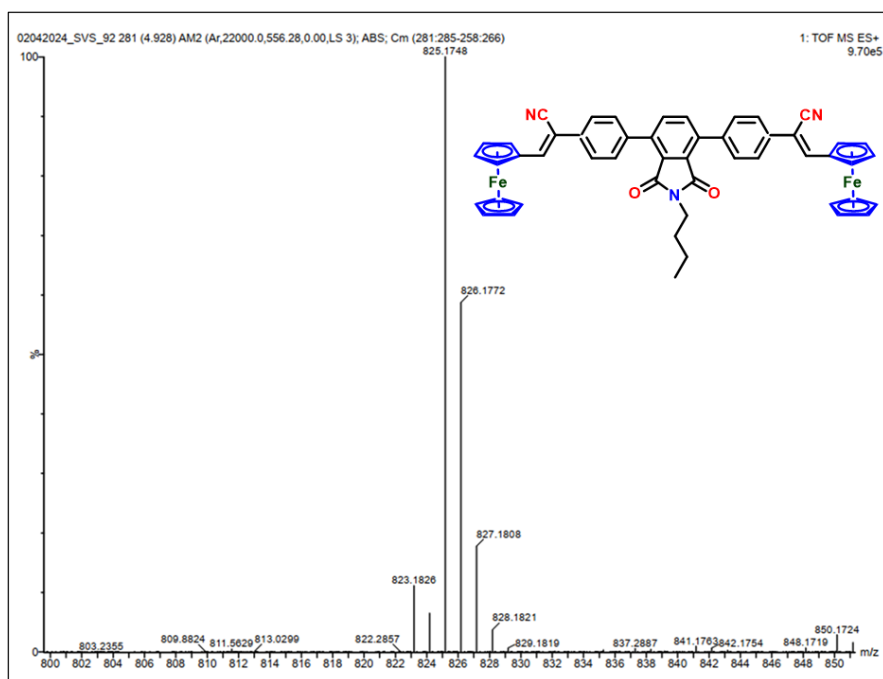
Fig. S9 HR-Mass spectra of the chromophore **2**
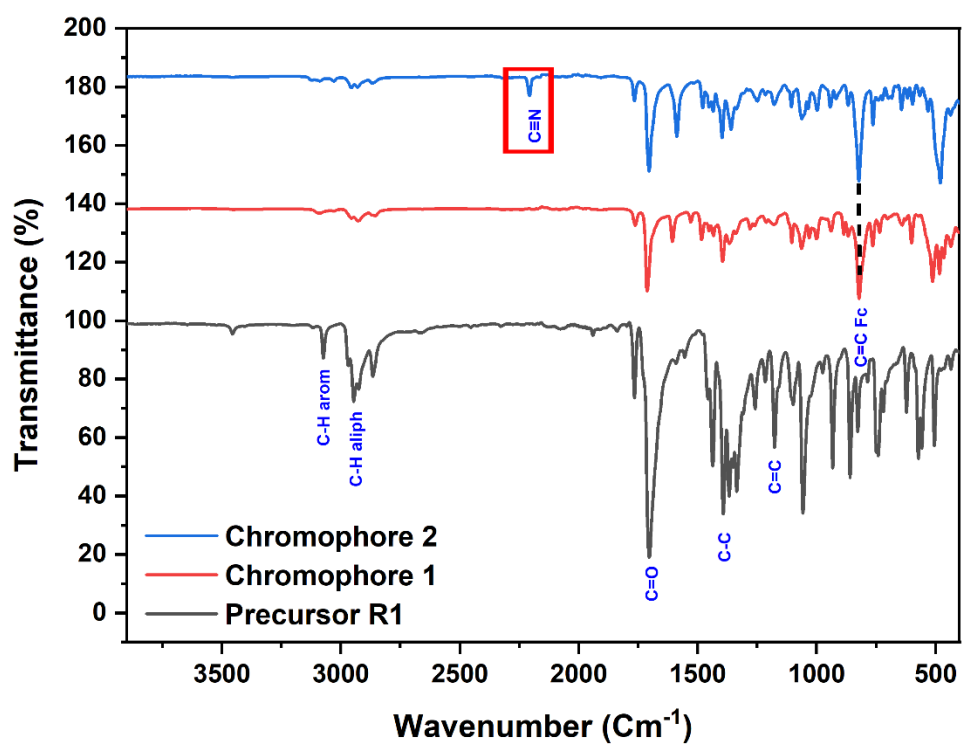
Fig. S10 FT-IR spectrum of the precursor **R1**, and the chromophores **1-2**
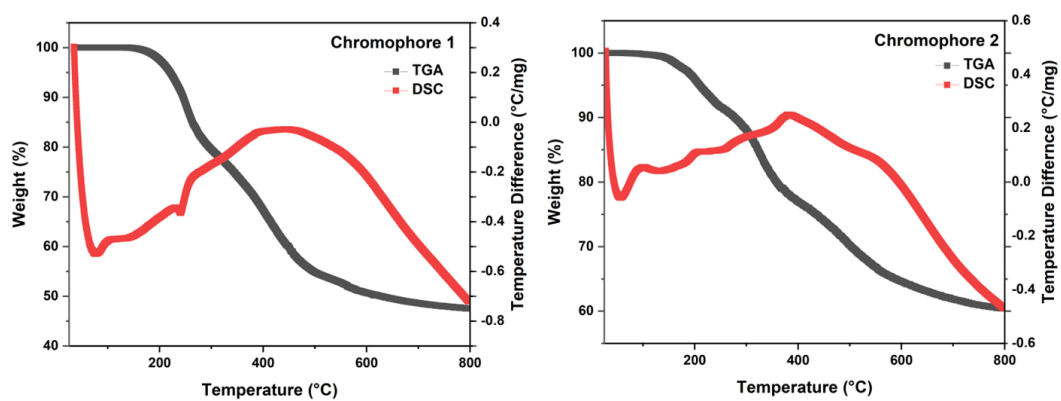
Fig. S11 TGA/DSC graph of the chromophores **1-2**
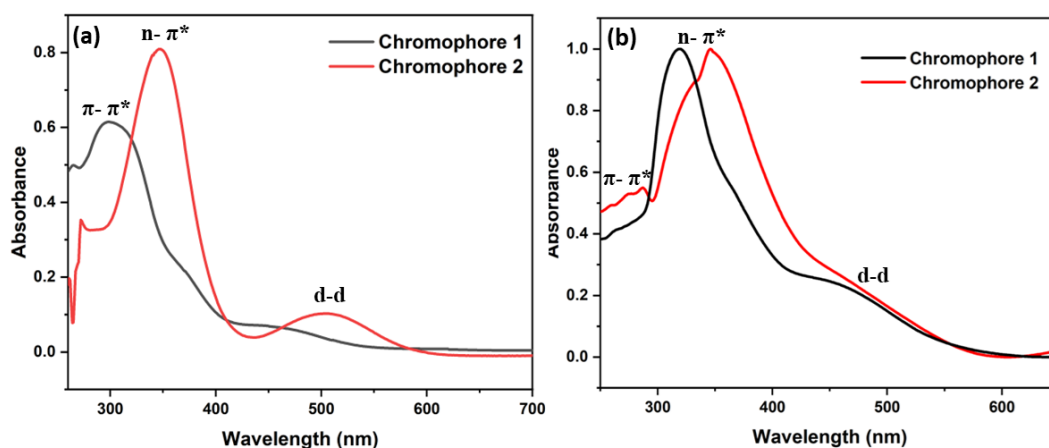
Fig. S12 Absorption spectra of the chromophores **1-2** (a) In chloroform solution (1×10^{-5}), (b) In thin film using PMMA binder.
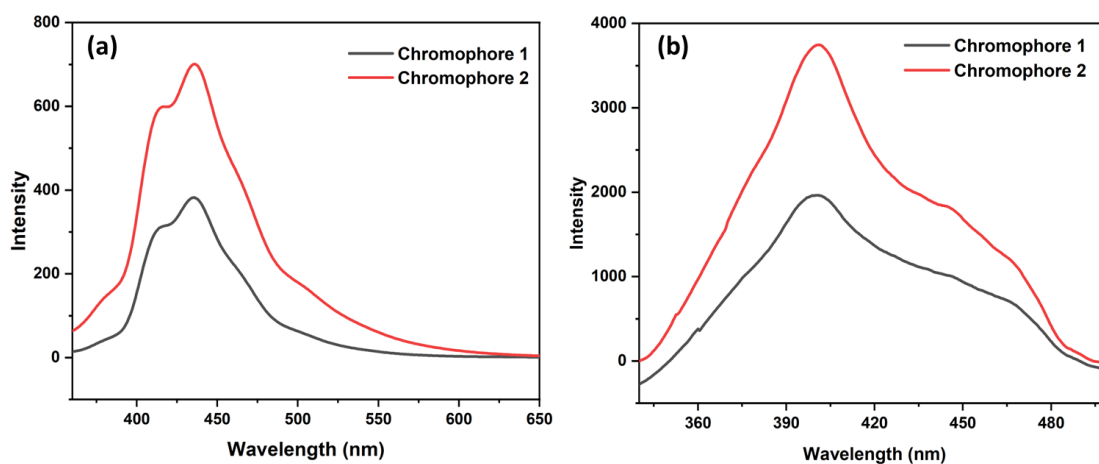
Fig. S13 Emission spectra of the chromophores **1-2** (a) In tetrahydrofuran solution (1×10^{-5}), (b) In thin film using PMMA binder.
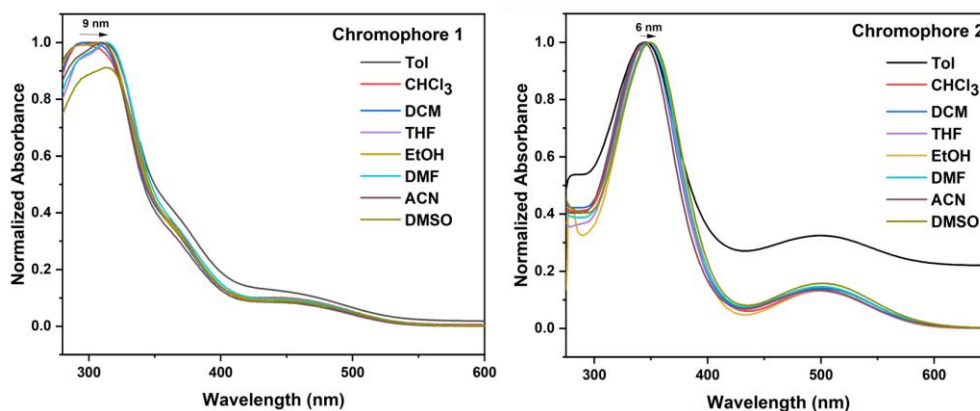
Fig. S14 UV-Visible spectra of chromophores **1** and **2** using various solvents (1×10^{-5} M)
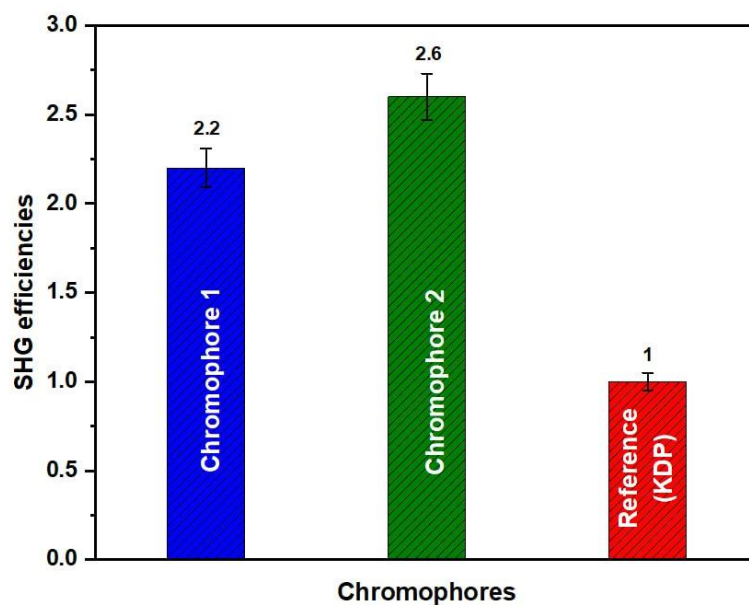
Fig. S15 Bar diagram of SHG efficiency of the chromophores **1-2**
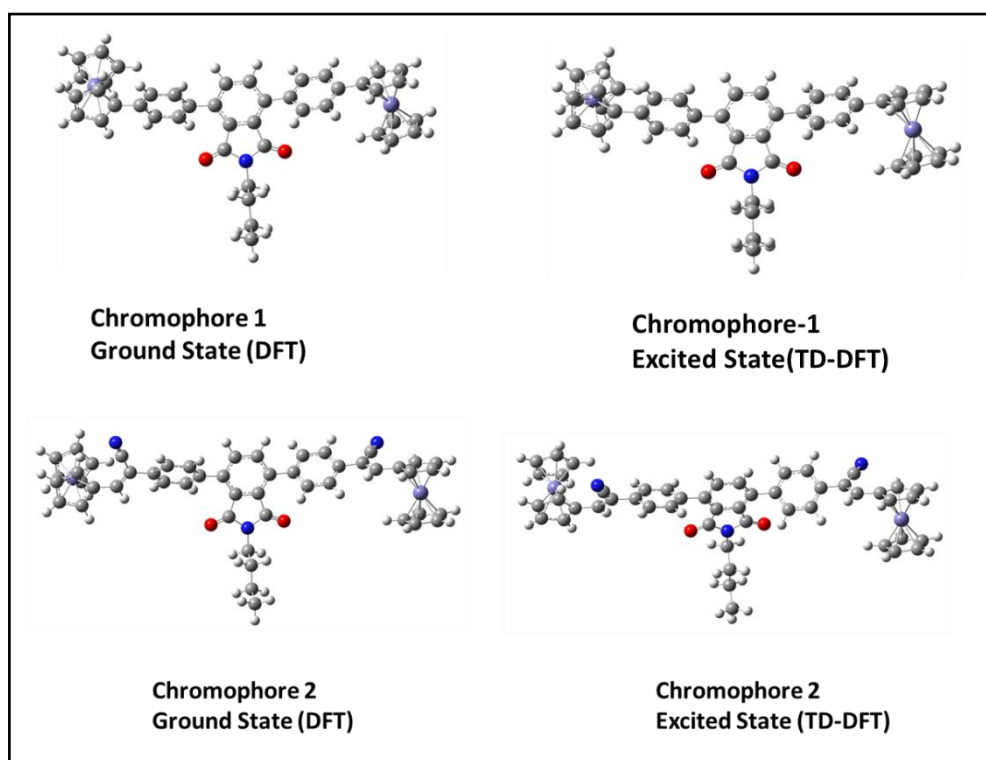
Fig. S16 The optimized geometries of chromophores **1-2** in ground and excited states attained theoretically *via* B3LYP/6-31+G** in CHCl$_3$ solvent
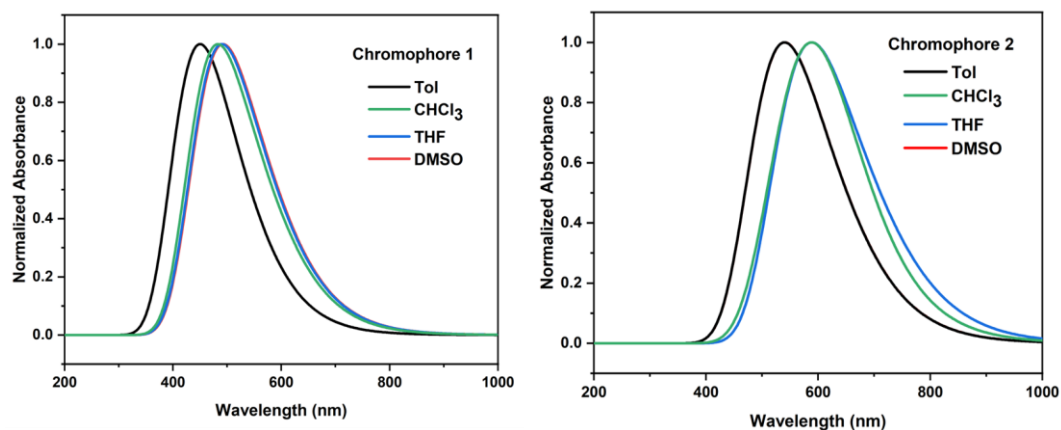
Fig. S17 Absorption spectra of the chromophores **1-2** in various solvents obtained at B3LYP/6-31+G** level of theory

Table S1 Crystallographic data and structural refinement of chromophore **2**

Identification code	Chromophore 2
CCDC	2368609
Empirical formula	$C_{50} H_{39} Fe_2 N_3 O_2$
Formula weight	825.54 g/mol
Temperature, K	300
Wavelength, Å	0.71073
Crystal System	Triclinic
Space group	P-1
Unit cell dimensions	a = 11.8348(9)Å, α = 106.557(3)°
	b =12.1373(10)Å, β =93.731(3)°
	c = 15.8828(12)Å, γ =113.053(3)°
Volume	1971.4(3)Å^3
Z	2
F (000)	856.0
Crystal size (mm^3)	0.04 x 0.17 x 0.28
Theta range for data collection (º)	1.91 to 27.91
Reflections collected	4765
Refinement method	Full-matrix least-squares on F2
R indices (all data)	R_1 = 0.0685, wR$_2$ = 0.1736

Table S2 Selected bond length (Å) and bond angles (°) of the chromophore **2** in crystal structure.

Selected bond length (Å)		Selected bond angles (°)	
Fe(1)-C(2)	2.070	C(2)-Fe(1)-C(4)	68.1
Fe(1)-C(6)	2.071	C(6)-Fe(1)-C(8)	67.8
C(1)-C(2)	1.426	C(5)-C(11)-C(12)	120.9
C(2)-C(3)	1.437	C(19)-C(23)-O(1)	129.6
C(5)-C(11)	1.476	C(21)-C(24)-O(2)	129.7
C(25)-N(1)	1.461	C(24)-N(1)-C(25)	123.9
C(23)-O(1)	1.220	C(14)-C(16)-C(17)	120.1
C(24)-O(2)	1.220	C(22)-C(23)-C(24)	120.0
Fe(2)-C(36)	2.065	C(29)-C(30)-C(31)	126.5
C(34)-C(35)	1.476	Fe(2)-C(32)-C(33)	69.8
C(22)-C(29)	1.486	C(35)-C(36)-Fe(2)	69.5

Table S3 Selected bond length (Å) and bond angles (°) of the chromophores **1-2** in DFT/ TD-DFT results in CHCl₃ solvent.

Selected bond length (Å) in Ground state/ Excited State		Selected bond angles (°) in Ground state/ Excited State	
Chromophore-1			
Fe(1)-C(2)	2.070/ 2.067	C(2)-Fe(1)-C(4)	68.1/ 62.7
Fe(1)-C(6)	2.071/ 2.069	C(6)-Fe(1)-C(7)	69.8/ 70.5
C(1)-C(2)	1.428/ 1.426	C(5)-C(11)-C(12)	120.9/ 121.0
C(5)-C(11)	1.476/ 1.475	C(16)-C(17)-C(18)	119.3/ 119.2
C(23)-O(1)	1.220/ 1.220	C(19)-C(23)-O(1)	129.6/ 129.7
C(24)-O(2)	1.220/ 1.220	C(21)-C(24)-O(2)	129.7/ 129.7
C(25)-N(1)	1.461/ 1.461	C(23)-N(1)-C(25)	124.0/ 123.9
Fe(2)-C(35)	2.083/ 2.220	C(29)-C(30)-C(32)	121.1/ 121.0
C(30)-C(32)	1.394/ 1.393	C(34)-C(35)-C(36)	126.5/ 126.1
C(43)-C(44)	1.429/ 1.428	Fe(2)-C(40)-C(41)	69.8/ 69.7
Chromophore-2			
Fe(1)-C(2)	2.077/ 2.088	C(2)-Fe(1)-C(4)	69.8/ 66.6
Fe(1)-C(6)	2.069/ 2.093	C(6)-Fe(1)-C(8)	69.6/ 66.4
C(1)-C(2)	1.423/ 1.424	N(1)-C(13)-C(12)	178.0/ 178.8
C(13)-N(1)	1.166/ 1.169	C(22)-C(25)-O(1)	129.6/ 129.3
C(39)-N(2)	1.166/ 1.169	C(26)-C(27)-O(2)	129.6/ 129.3
C(28)-N(3)	1.462/ 1.462	C(28)-N(3)-C(25)	123.9/ 123.9
C(25)-O(1)	1.220/ 1.220	C(16)-C(18)-C(19)	121.0/ 120.8
C(27)-O(2)	1.220/ 1.220	C(33)-C(35)-C(37)	120.9/ 120.6
Fe(2)-C(49)	2.076/ 2.100	N(2)-C(39)-C(38)	177.9/ 177.4
C(16)-C(18)	1.429/ 1.420	Fe(2)-C(42)-C(43)	70.5/ 69.8
C(33)-C(35)	1.423/ 1.394	C(48)-C(49)-Fe(2)	69.6/ 69.6

Table S4 Dihedral angle results of the chromophores **1-2** in crystal structure, DFT/TD-DFT results in CHCl$_3$ solvent.

Atoms	Dihedral angle (Crystal structure)/ Deviation of dihedral angle from the plane	Dihedral Angle (DFT-Ground state)/ Deviation of dihedral angle from the plane	Dihedral Angle (TD-DFT-Excited state)/ Deviation of dihedral angle from the plane	Deviation of dihedral angle between ground and excited state
Chromophore-1				
C14-C7-C6-C19	-	126.59 °/ 53.41°	128.23 °/ 51.77 °	1.64 °
C16-C7-C6-C8	-	130.85 °/ 49.15°	132.32 °/ 47.68 °	1.47 °
C10-C9-C17-C27	-	130.88 °/ 49.12 °	132.56 °/ 47.44 °	1.68 °
C23-C9-C17-C21	-	127.49 °/ 52.51 °	128.43 °/ 51.57 °	0.94 °
Chromophore-2				
C17-C19-C20-C21	130.93 ° /49.07 °	-154.18 °/ 25.82 °	-132.23 °/ 47.77 °	21.95 °
C23-C24-C32-C34	143.30 ° /36.70 °	130.85 °/ 49.15 °	115.58 °/ 64.42 °	15.27 °
C36-C37-C38-C39	158.67 ° /21.33 °	127.49 °/ 52.51 °	110.86 °/ 69.14 °	16.63 °
C13-C12-C14-C15	151.77 ° /28.23 °	155.50 °/ 24.50 °	139.21 °/ 40.79 °	16.29 °

Table S5 Electrochemical data of the chromophores **1-2**

S.no	E_{pa} (mV)[a]	E_{pc} (mV)[a]	i_{pc}/i_{pa} (V)[a]	$E_{1/2}$ (mV)[a]	ΔE (mV)[a]	E_{HOMO} (eV)[a]	E_{LUMO} (eV)[a]	$E_g^{optical}$ (eV)[b]
1	598	290	0.71	444	308	-4.99	-1.70	3.29
2	794	527	0.63	660	267	-5.19	-1.06	4.13

[a]Calculated HOMO and LUMO energy levels attained from the cyclic voltammetry using the equation E_{HOMO} = −e (E_{ox}+4.4), E_{LUMO} = $E_g^{optical}$ + E_{HOMO}
[b]Calculated λ^{onset} value observed in absorption spectra in CHCl$_3$ solvent [(358 nm (**1**), 370 nm (**2**)]
[b]Optical band gap value was calculated from absorption onset, using the equation $(E_g^{optical})$ = 1240/λ^{onset}

Table S6 Photophysical data of the chromophores **1-2** in solution (CHCl$_3$) and thin film

S.no	Absorption Spectra Solution/ Thin film			Emission Spectra Solution/ Thin film	
	π-π* (nm)	n-π* (nm)	d-d (nm)	$\lambda_{excitation}$ (nm)	$\lambda_{emission}$ (nm)
1	275/281	360/319	458/464	280/280	419/400
2	274/287	376/348	505/474	280/280	417/401
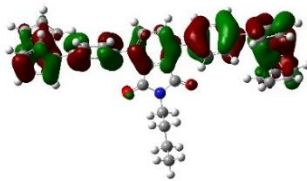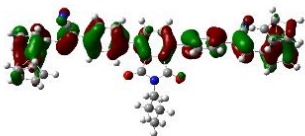
Table S7 Solvatochromic properties of chromophores **1** and **2**
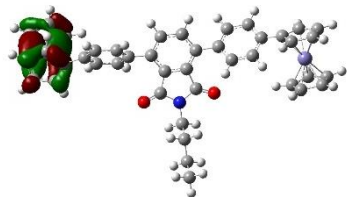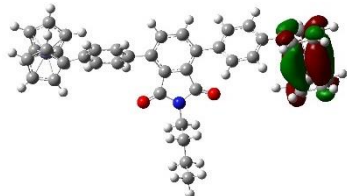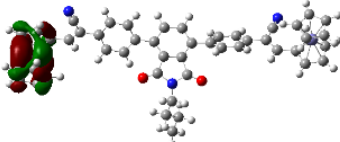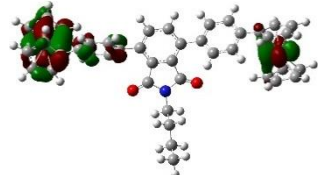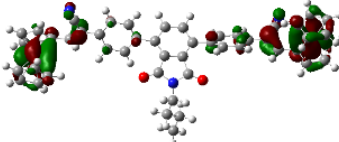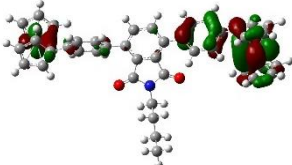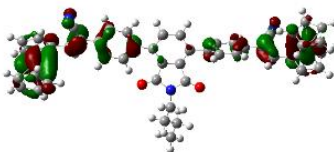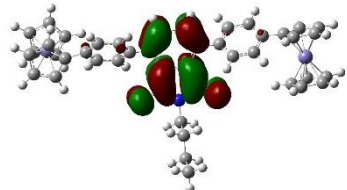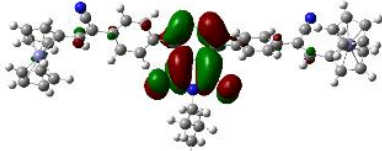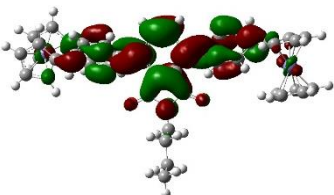
Solvents	UV-Visible $^a\lambda_{max}$ (nm)		Fluorescence $^a\lambda_{max}$ (nm)	
	Chromophore-**1**	Chromophore-**2**	Chromophore-**1**	Chromophore-**2**
Toluene	311	344	409	412
CHCl₃	309	346	415	425
DCM	311	345	416	436
THF	314	346	431	433
EtOH	315	347	427	427
ACN	317	347	432	428
DMF	319	348	431	432
DMSO	320	348	434	439

Table S8 Selected transitions attained theoretically (TD-DFT, Excited state-CHCl₃) for the chromophores **1-2** calculation in B3LYP/6-31+G**

Entry	λ (nm)	Oscillator strength, f	Energy (eV)	Selected Major Transitions[a]
Chromophore 1	476	0.0103	2.60	H-1 → L (86%)
	461	0.0001	2.68	H-3 → L (94%)
	401	0.0298	3.08	H-4 → L (95%)
Chromophore 2	454	0.0073	2.72	H → L (92%)
	425	0.0001	2.91	H-2 → L (89%)
	424	0.0001	2.91	H-3 → L (90%)

Values are calculated in CHCl₃ solution. [a]Only components with contributions greater than 80% are shown. Percentage contribution approximated by $2(c_i)^2(100\%)$, where c_i is the coefficient for the particular orbital rotation.
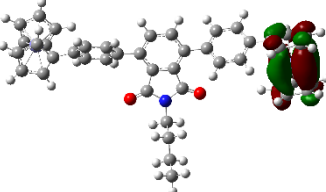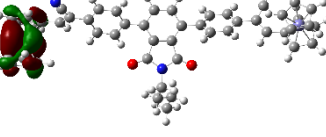
Table S9 The density surfaces (frontier orbitals) involved in electronic transitions of the chromophores **1-2** attained theoretically (TD-DFT, Excited state-Toluene) derived from B3LYP/6-31+G**

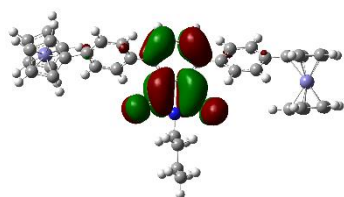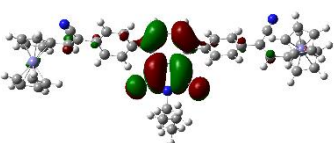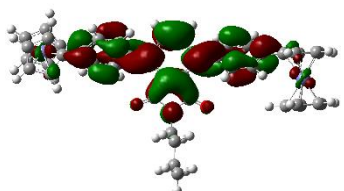| Orbitals	Chromophore 1	Chromophore 2
HOMO-4		

HOMO-3		
HOMO-2		
HOMO-1		
HOMO		
LUMO		
LUMO+1		
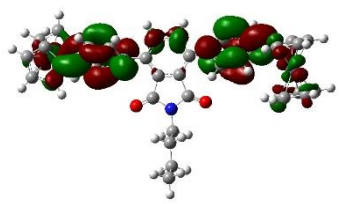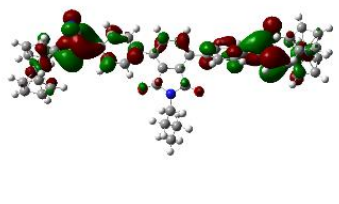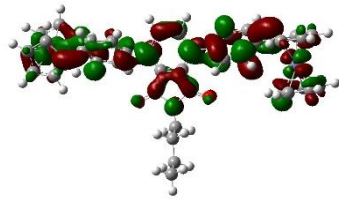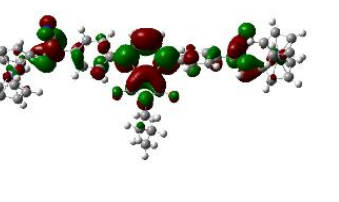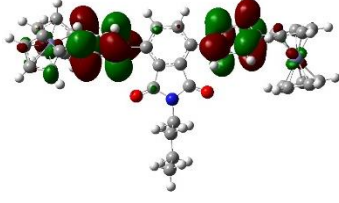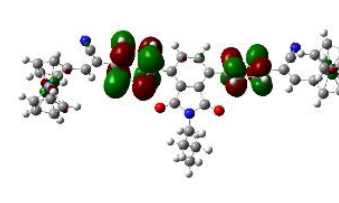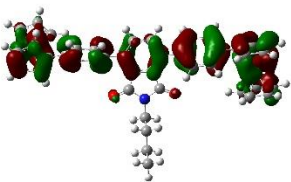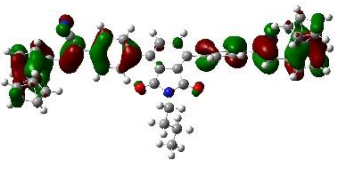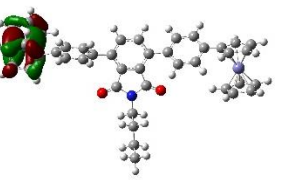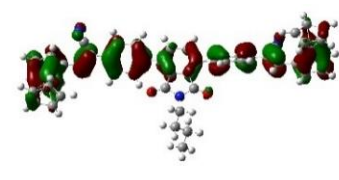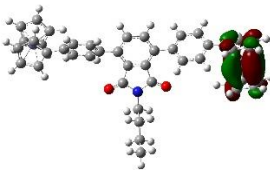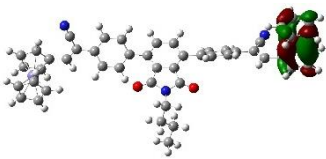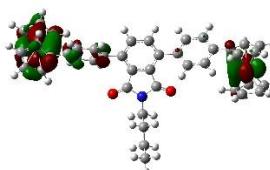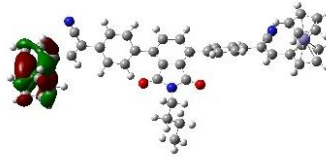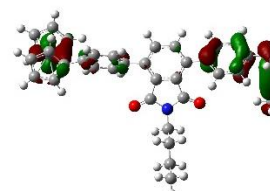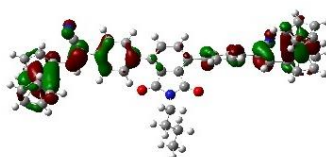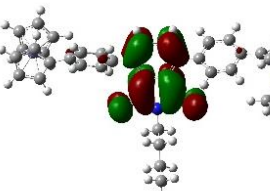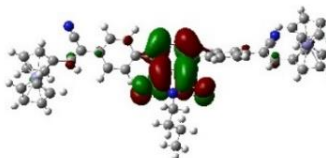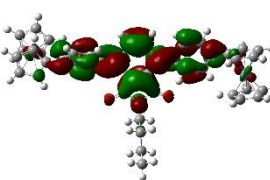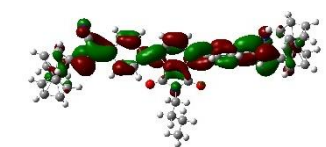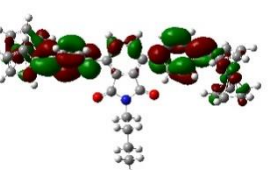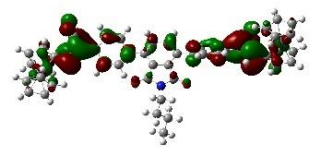
Orbitals	Chromophore 1	Chromophore 2
LUMO+2		
LUMO+3		
LUMO+4		

Table S10 The density surfaces (frontier orbitals) involved in electronic transitions of the chromophores **1-2** attained theoretically (TD-DFT, Excited state-CHCl$_3$) derived from B3LYP/6-31+G**

Orbitals	Chromophore 1	Chromophore 2
HOMO-4		
HOMO-3		

HOMO-2		
HOMO-1		
HOMO		
LUMO		
LUMO+1		
LUMO+2		
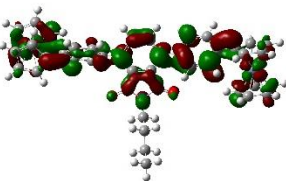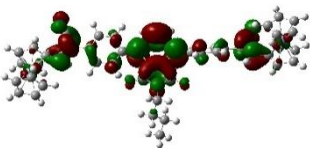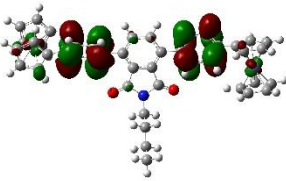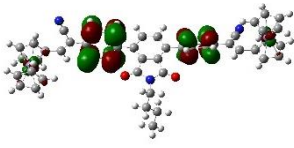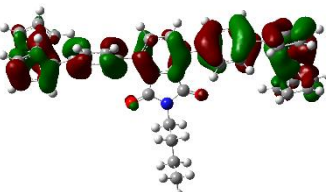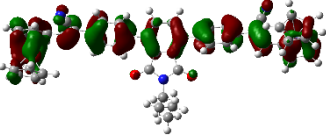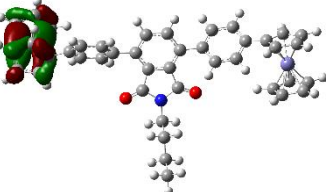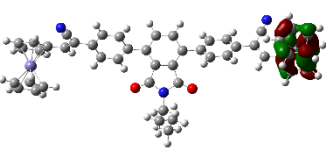
LUMO+3		
LUMO+4		

Table S11 The density surfaces (frontier orbitals) involved in electronic transitions of the chromophores **1-2** attained theoretically (TD-DFT, Excited state-THF) derived from B3LYP/6-31+G**

Orbitals	Chromophore 1	Chromophore 2
HOMO-4		
HOMO-3		
HOMO-2		
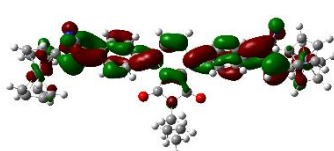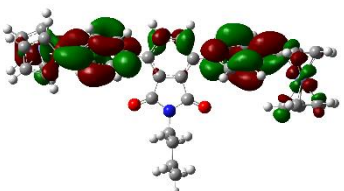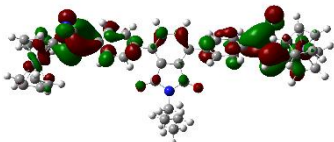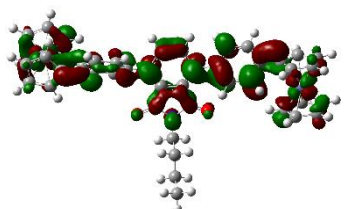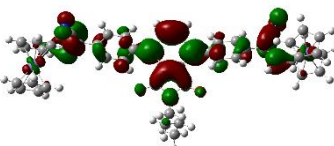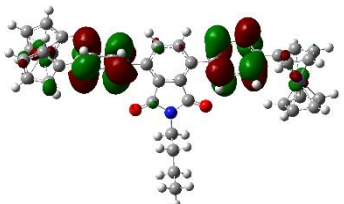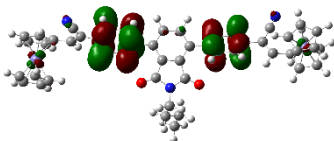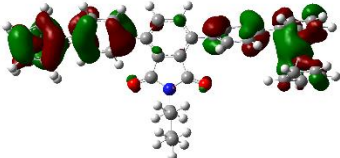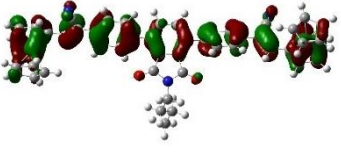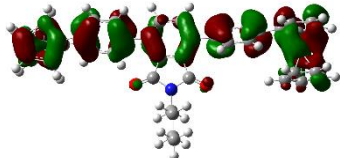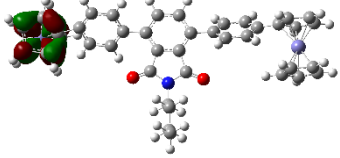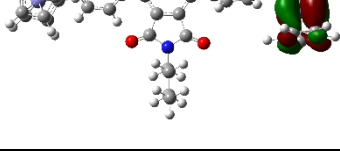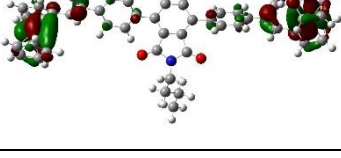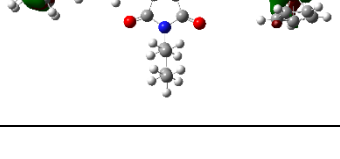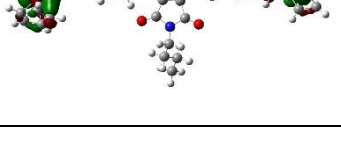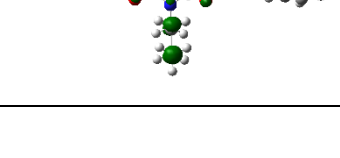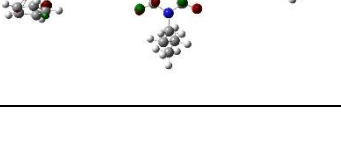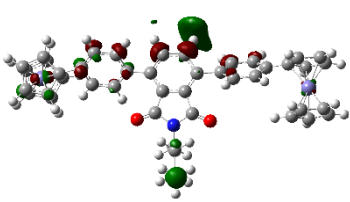
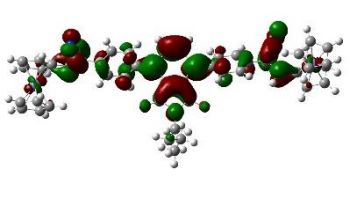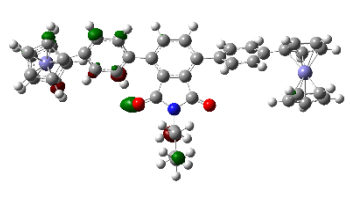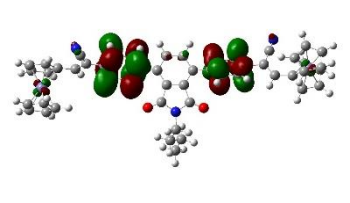|		
LUMO		
LUMO+1		
LUMO+2		
LUMO+3		
LUMO+4		

Table S12 The density surfaces (frontier orbitals) involved in electronic transitions of the chromophores **1-2** attained theoretically (TD-DFT, Excited state-DMSO) derived from B3LYP/6-31+G**

Orbitals	Chromophore 1	Chromophore 2
HOMO-4		
HOMO-3		
HOMO-2		
HOMO-1		
HOMO		
LUMO+2		

LUMO+3		
LUMO+4		

Reference

1. 1. P. Solanke, F. Bureš, O. Pytela, J. Kulhánek and Z. Padělková, *Synthesis (Stuttg).*, 2013, **45**, 3044–3051.

2. T. Viswanathan and N. Palanisami, *New J. Chem.*, 2021, **45**, 12509–12518.

3. G. M. Sheldrick, SHELXS version-2018/3 and SHELXL version-2018/3, 2018.

4. J. Heinze, J, *Angew. Chem. Int. Ed.,* 1984, **23**, 831-847.

5. S. K. Kurtz and T. T. Perry, *J. Appl. Phys.*, 1968, **39**, 3798–3813.

6. A. D. Becke, *Phys. Rev. A*, 1988, **38**, 3098.

7. M. J. Frisch, G. W. Trucks, H. B. Schlegel, G. B. Scuseria, M. A. Robb, J. R. Cheeseman and D. J. Fox, *Gaussian Inc. Wallingford CT,* 2016, **1**, 572.

8. O. Christiansen, J. Gauss and J. F. Stanton, *Chem. Phys. Lett.,* 1999, **305**, 147-155.